III-5

Life, Earth and Planetary Sciences

BL1U

Circularly Polarized Lyman-α Light Irradiation on Racemic Amino Acid Film to Verify the Cosmic Scenario of Origin of Homochirality

M. Kobayashi[1], K. Matsuo[2], M. I. A. Ibrahim[2], H. Chimura[1], J. Takahashi[3], K. Shimizu[4], H. Ota[4,5], Y. Satake[6], T. Minato[7], N. Takada[7], G. Fujimori[7], K. Kobayashi[8,9], Y. Kebukawa[9], M. Katoh[2,4] and H. Nakamura[1,6]

[1]*National Institute for Fusion Science, Toki city 509-5292, Japan*
[2]*Reserach Institute for Synchrotron Radiation Science, Hiroshima Univ., Higashi-Hiroshima 739-0046, Japan*
[3]*Graduate School of Maritime Sciences, Kobe University, Kobe 658-0022, Japan*
[4]*UVSOR Synchrotron Facility, Institute for Molecular Science, Okazaki city 444-8585, Japan*
[5]*Japan Synchrotron Radiation Research Institute, 1-1-1, Kouto, Sayo-cho, Sayo-gun, Hyogo 679-5198, Japan*
[6]*Nagoya University, Furo-cho, Chikusa-ku, Nagoya 464-8601, Japan*
[7]*Institute for Molecular Science, Okazaki city 444-8585, Japan*
[8]*Department of Chemistry and Life Science, Yokohama National University, Yokohama 240-8501, Japan*
[9]*Department of Earth and Planetary Sciences, Institute of Science Tokyo, Meguro-ku, Tokyo 152-8550 Japan*

The homochirality of life remains one of the most enigmatic issues in the study of the origin of life. A proposed mechanism for symmetry breaking involves irradiation by circularly polarized light (CPL). To investigate the photoreaction of amino acids induced by vacuum ultra-violet (VUV) CPL irradiation, we performed experiments where amino acids in a solid state were irradiated with CPL. This study focuses on Lyman-α (121.6 nm in wavelength), a leading candidate for selective photolysis when circularly polarized.

To investigate the photoreaction of amino acids caused by VUV CPL irradiation, we developed a VUV CPL irradiation system at the beamline BL1U in UVSOR at the Institute for Molecular Science [1]. Lyman-α CPL was generated in BL1U, and racemic alanine film specimens were irradiated with this CPL beam. After irradiation, distinct optical activity was observed, with positive and negative values of the optical anisotropy factor for right-handed (R) -CPL and left-handed (L) -CPL irradiation, respectively. However, the anisotropy factor spectra are broad in the measured wavelength range of 180–240 nm, differing from those of enantiopure alanine samples [1]. These results suggest that Lyman-α CPL irradiation not only caused simple preferential photolysis of enantiopure alanine molecules but also introduced additional effects such as oligomerization or polymerization.

These effects were corroborated by LC-MS analysis. The non-irradiated alanine sample predominantly displayed a single peak corresponding to the protonated alanine monomer $[Ala + H]^+$ (NH_3^+-$CHCH_3$-COOH) of m/z = 90. In contrast, the Lyman-α light-exposed samples exhibited additional complex peaks, which suggest the formation of larger molecules, such as oligomeric alanine adducts or modified oligomers, as inferred from their fragmentation patterns with high abundances of m/z values in the range 170 – 450.

It was also observed that Lyman-α CPL irradiation induced the formation of circular network ag-aggregates on the order of 100 nm in the surface of the alanine film with scanning probe microscopy (SPM) measurements, as shown in Fig.1. These results may suggest dimerization, polymerization, or micro-crystallization induced by the high photon energy of the Lyman-α CPL. Further investigations are ongoing to study the photoreaction of amino acids caused by VUV CPL irradiation.

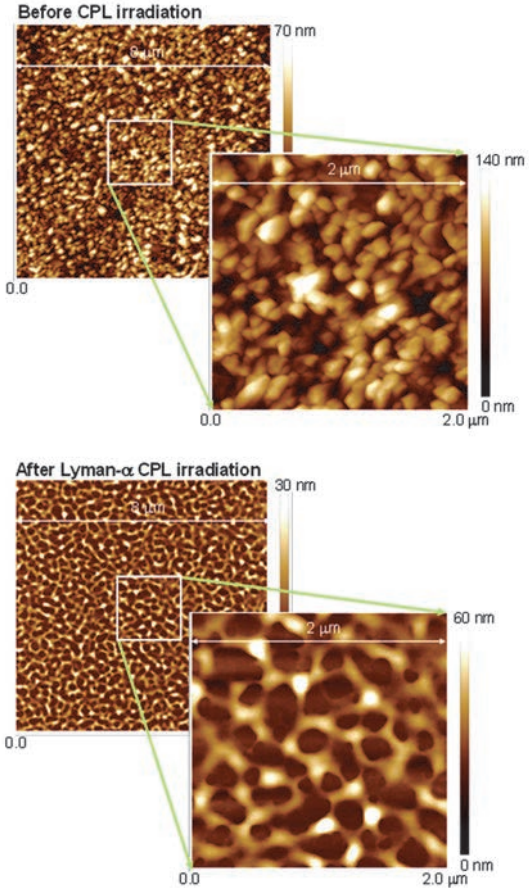

Fig. 1. Topographic images of the DL-alanine film obtained by SPM before (upper) and after (lower) CPL irradiation.

[1] M. Kobayashi *et al.,* Chirality **36** (2024) e70004.

BL1U

Experimental and Theoretical Studies Towards Observing Interactions between Biomolecules and Ultraviolet Optical Vortex

K. Matsuo[1,3,4], H. Kawaguchi[2], R. Imaura[3], S. Hashimoto[3], Y. Nishihara[4], H. Ota[5] and M. Katoh [1,3,4,5]

[1]*Reseach Institute for Synchrotron Radiation Science, Hiroshima University, Higashi-Hiroshima 739-0046, Japan*
[2]*Muroran Institute of Technology, Muroran 050-8585, Japan*
[3]*Graduate School of Advanced Science and Engineering, Hiroshima University, Higashi-Hiroshima 739-8526, Japan*
[4]*School of Science, Hiroshima University, Higashi-Hiroshima 739-8526, Japan*
[5]*UVSOR Synchrotron Facility, Okazaki 444-8585, Japan*

Chirality is an important structural factor in understanding the properties and functions of materials. Circular dichroism spectroscopy using right- and left-handed circularly polarized light with spin angular momentum (SAM: *s*) can observe the chirality of biomolecules in the ultraviolet region below 300 nm. On the other hand, right- and left-handed optical vortex with orbital angular momentum (OAM: *l*) are also expected to be a method for observing chirality, but there are few reports of observations of the interaction between the chirality of biomolecules and optical vortex [1-3], because a method for generating optical vortex in the ultraviolet region has not been established. In this study, in order to observe the interaction between an ultraviolet optical vortex and a biomolecule, we constructed an experimental system which can monitor the ultraviolet absorption of optical vortex using a synchrotron radiation undulator [4-5], and theoretically verified the interaction between an optical vortex and a chiral structure using a finite-difference time-domain method [6].

The second-harmonic light from the helical undulator, which is circularly polarized optical vortex ($s = l = +1$; $s = l = -1$) in the ultraviolet region, is introduced to an optical system consisting of a sample holder, a focusing lens, and a mini-monochromator, which enable the absorption measurement of the circularly polarized optical vortex. To confirm the generation of an optical vortex in the ultraviolet region, a triangular aperture was placed at the sample position, and the optical image was observed with a CCD camera, revealing characteristic scattering patterns indicating right- and left-handed optical vortex [7].

As a chiral sample, the absorption of right- and left-handed optical vortex of + (plus) and – (minus) type *10* camphorsulfonic acid (CSA) was observed at 290 nm. Both the circular dichroism and helical dichroism (Differences in absorbance between right- and left-handed optical vortex) of CSA showed positive and negative values for the + and – types, respectively, but an increase in the intensity of the helical dichroism was observed.

Using the moment method, a type of finite-difference time-domain method, we placed a helical coil at the center of a circularly polarized optical vortex field (or circularly polarized field) (Fig. 1) and theoretically observed the helical dichroism (or circular dichroism) from the scattering intensity of the interaction between the optical vortex (or circularly polarized light) and the coil. With a single coil, the intensity of the helical dichroism was smaller than the circular dichroism, but with two or three parallel coils, the difference between the helical and circular dichroism became smaller. Furthermore, when one coil was moved to the radial direction from the center point of the vortex field, the difference between the helical and circular dichroism became smaller. These theoretical results suggest that the position of a chiral sample relative to the optical vortex field strongly affects their interaction, and indicate the need to take the sample position into account when measuring optical vortex absorption.

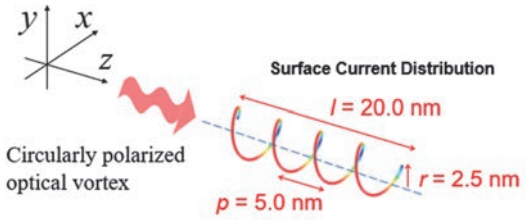

Fig. 1. Helical coil at the center of a circularly polarized optical vortex field for theoretical calculations of helical dichroism (or circular dichroism).

[1] Brullot *et. al.*, Sci. Adv. **2** (2016) e1501349.
[2] Ni *et. al.*, ACS Nano **15** (2021) 2893.
[3] Rouxel *et. al.*, Nat. Photonics **16** (2022) 570.
[4] Katoh *et. el.*, Sci. Rep. **7** 6130 (2017) & Phys. Rev. Lett. **118** (2017) 094801.
[5] Kaneyasu and Katoh *et. al.*, Phys. Rev. A, **95** (2017) 023413.
[6] Kawaguchi, Int. J. Appl. Electromagn. Mech., **65** (2021) 17.
[7] Y. Nishihara *et al.*, UVSOR Activity Report **51** (2024) 47.

BL4U

X-ray Absorption Spectroscopic Analysis of Spatial Distribution of Water Molecules in Deep-Sea White Smoker Chimney Minerals

H. E. Lee[1], T. Araki[2] H. Takahashi[1], and A. Koishi[3]
[1]*Editorial Board, Earth-Life Science Institute (ELSI), Institute of Science Tokyo, Tokyo 152-8550, Japan*
[2]*UVSOR Synchrotron Facility, Institute for Molecular Science, Okazaki 444-8585, Japan*
[3]*RIKEN Center for Sustainable Resource Science, Wako, Saitama 351-0198 Japan*

This study successfully conducted the world's first spatially-resolved soft X-ray absorption spectroscopy (STXM) analysis on minerals collected from the White Smoker Chimney located in the Mariana Trench (depth: 5743 meters)[1]. The primary aim was to investigate the chemical state and two-dimensional spatial distribution of water molecules within the nano-confined spaces of $Mg(OH)_2$ based mineral structures that constitute the chimney. Utilizing the oxygen K-edge spectra, the measurements allow us to map the presence and orientation of water molecules under both dry and humidified conditions.

Our findings reveal that water confined in the nanoscale environments created by oriented $Mg(OH)_2$ exhibits distinct molecular orientations and hydrogen bonding characteristics that differ markedly from bulk water. These altered properties are critical because they suggest the possibility of facilitating dehydration-condensation reactions, such as those involved in the formation of peptides or nucleic acids, which are generally inhibited in bulk aqueous environments. This insight directly addresses the long-standing "Water Paradox" in the origin of life research, where water is essential for life but simultaneously suppresses key synthetic reactions[2].

By employing a soft X-ray beam at BL4U (UVSOR), the study achieved high resolution in visualizing the distribution of water at the nanoscale in a wet environment. The spectroscopic features observed in the pre-edge (~535 eV), main-edge (~537 eV), and post-edge (~540 eV) regions provided detailed information on the saturation level of hydrogen bonds and surface interactions. An increased peak intensity was observed around 536~537 eV, which is expected to be associated with the characteristics of confined water[3].

As only a few research groups worldwide possess samples from the White Smoker Chimney, the structural and chemical insights provided by this study are both novel and significant. The experimental techniques developed and applied here offer a powerful platform for future exploration of water–mineral interactions and their role in supporting life-like chemical processes in extreme environments. This research not only opens new avenues in catalytic chemistry by highlighting the functional potential of mineral-bound nano-confined water but also contributes fundamentally to the field of prebiotic chemistry and the study of life's origins.

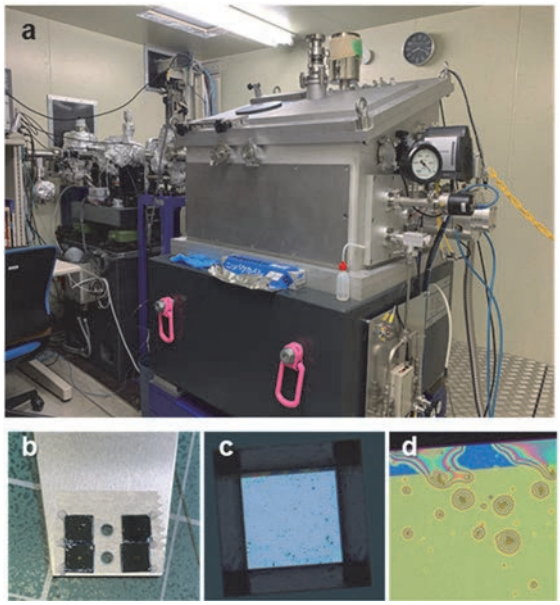

Fig. 1. a. Photograph of the STXM setup at UVSOR. b. Wet cell mounted on the sample holder. c, d. Samples enclosed within a wet cell, prepared by sandwiching them between two SiNx windows.

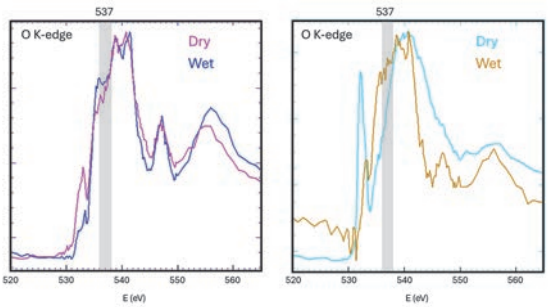

Fig. 2. O K-edge spectra of two different samples with wet and dry conditions.

[1] H.-E. Lee *et al.*, Nat. Commun. **15** (2024) 8193.
[2] M. Marshall, Nature **588** (2020) 210.
[3] K. Yamazoe *et al.*, Langmuir **33** (2017) 3954.

BL4U

Nocturnal Aerosol Growth in New Delhi – A Microscopic Investigation

M. Wickramanayake[1], E. Tsiligiannis[1], T. Araki[2] and X. Kong[1]
[1]*Department of Chemistry and Molecular Biology, University of Gothenburg, SE-412 96 Gothenburg, Sweden*
[2]*UVSOR Synchrotron, Institute for Molecular Science, Okazaki 444-8585, Japan*

This study explores the nighttime growth of atmospheric aerosol particles in New Delhi, one of the most polluted megacities globally, using advanced synchrotron-based techniques. The research addresses a significant knowledge gap in understanding the molecular composition and growth mechanisms of aerosols [1], particularly during nocturnal hours in winter when air pollution events intensify [2]. Sampling was conducted in February and March 2023 from the rooftop of the Indian Institute of Technology (IIT) Delhi, and analytical measurements were carried out at the UVSOR-III synchrotron facility in Japan in March 2024. The primary tools used were Scanning Transmission X-ray Microscopy (STXM) and Near Edge X-ray Absorption Fine Structure (NEXAFS) spectroscopy, enabling high-resolution imaging and chemical speciation of individual aerosol particles.

This investigation examines the diurnal variation of aerosol particle morphology and composition in New Delhi using STXM images at 300 eV, an energy optimal for detecting carbonaceous materials. Three particle types were identified by color: black (carbon- rich soot), grey (inorganics like potassium), and mixed (organic-inorganic combinations). Black particles often appeared chain-like, grey ones polygonal, and mixed particles suggested internal mixing due to condensation or fog processing.

Figure 1 captured during four different conditions (polluted day, clean day, polluted night, and clean night) show significant changes in particle abundance and morphology. Notably, the nighttime images showed a higher degree of spherical structures and internal mixing, supporting the idea of aqueous-phase processing under high humidity conditions, which is common at night in winter.

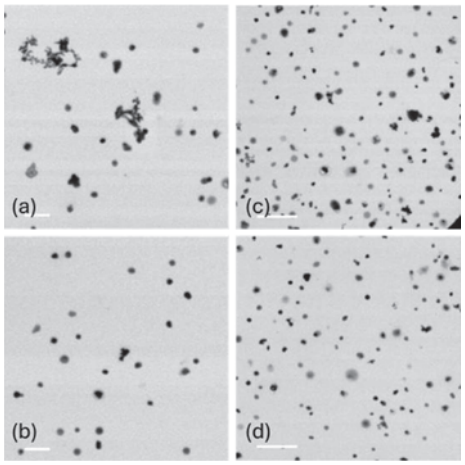

Fig. 1. STXM images of particle morphology during (a) polluted day, (b) clean day, (c) polluted night, and (d) clean night. The scale bar of each is in the bottom left corner showing as a white strip, where (a) and (b) are 2 μm, (c) and (d) are 5 μm.

A key observation lies in the change in particle composition. During both night conditions, the proportion of mixed particles increased, while the number of black (carbonaceous) particles decreased. In the polluted scenario, mixed particles increased by 13%, while black particles dropped by 8% and grey particles by 5%. For the clean scenario, the increase in mixed particles was even more prominent (15%) while grey particles rose by 13%, and black particles showed a sharp 28% decline. This suggests that nighttime conditions favor the transformation of pure carbonaceous or inorganic particles into more internally mixed forms, likely due to condensation of organic vapors and moisture.

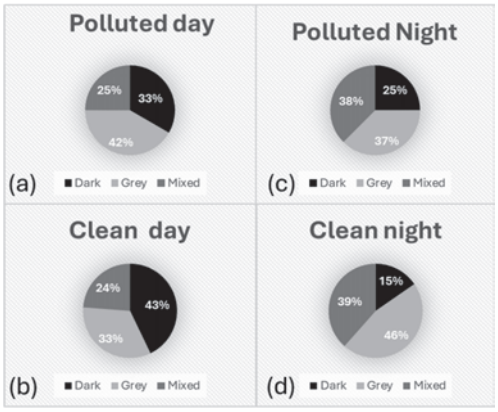

Fig. 2. The fractions of particles distributed into three categories.

The mixing state, which influences how particles interact with solar radiation and water vapor, shifts notably at night. The presence of internally mixed, spherical particles suggests fog or aqueous-phase processing, where particles absorb or coat one another, altering their chemical composition. This affects both climate forcing and health, as internally mixed particles have different optical and hygroscopic properties than externally mixed ones. STXM image analysis and particle count data show that nighttime conditions in New Delhi led to more internally mixed aerosols with larger sizes and distinct compositions. These changes are driven by lower temperatures, higher humidity, and emissions from biomass burning. The results underscore the need to consider diurnal variation in air quality assessments and control strategies.

[1] M.Hallquist *et al.*, Atmos. Chem. Phys. **9** (2009) 5155.
[2] J. K. Kodros *et al.*, PNAS **117** (2020) 33028.

III-5

BL4U

Trial of Molecular Mapping for Thin Sections of Isolated Mammalian Nuclei Embedded in Paraffin Using STXM

A. Ito[1], K. Shinohara[2], A. Matsuura[2], S. Toné[3], S. Ohira[4], A. Nagai[4], Y. Asada[2], T. Ohigashi[5], H. Yuzawa[6] and T. Araki[6]

[1]*School of Engineering, Tokai University, Hiratsuka 259-1292, Japan*
[2]*Graduate School of Health Sciences, Fujita Health University, Toyoake 470-1192, Japan*
[3]*School of Science and Engineering, Tokyo Denki University, Hatoyama 350-0394, Japan*
[4]*Kawasaki Medical School, Kurashiki 701-0192, Japan*
[5]*Photon Factory, Institute of Materials Structure Science, Tsukuba 305-0801, Japan*
[6]*UVSOR Synchrotron Facility, Institute for Molecular Science, Okazaki 444-8585, Japan*

Spectromicroscopy using STXM is one of the most effective tools for molecular mapping at high spatial resolution. For the application to biological specimens, we have developed an image processing method for a quantitative distribution of constituent molecules, and successfully obtained molecular images in chromosomes, mammalian cells, and mammalian isolated normal and apoptotic nuclei [1-3]. However, due to low transmission of soft X-rays to thick areas in the isolated nucleus, reliable analysis for molecular distribution could not be achieved [3]. To try to solve this problem, thin sections of isolated nuclei with the thickness around 200 nm were prepared by embedding in resin [4]. Although the transmission was greatly improved, we could not exclude the possibility that significant amount of resin in the sections might interfere in the analysis for molecular distribution. In the present study, we adopted paraffin in place of resin, because paraffin in the thin section can be removed by soaking in xylene. In contrast, paraffin section is not so thin as resin section; around 2 μm thickness would be lower limit of the thickness. This report is the first preliminary results using paraffin embedded section.

Isolated nuclei from human HeLa S3 cells were fixed with glutaraldehyde followed by mixing with agarose to confine to a limited volume, and then embedded in paraffin. The paraffin sections were prepared with thicknesses of 5, 3 and 2 μm, and found that 2 μm was the best choice from the transmitted intensity. The section was attached directly on SiN membrane and then soaked in xylene to remove paraffin from section samples.

We basically applied the SVD (Singular Value Decomposition) method to obtain molecular distributions [3]. Energy stack images obtained at the C, N and O-K edges were analyzed using NEXAFS spectra of nucleic acids (DNA and RNA), proteins (histone and actin), and agarose.

Figure 1a shows an X-ray transmission image of a 2 μm-thick thin section of an isolated nucleus observed at 285 eV, where the dense area in the center of nucleus may be assigned to be a nucleolus. The image has somewhat irregular jagged boundary, which may result from sectioning technique of challenging thin thickness. Molecular images of DNA, RNA, histone, and actin were shown in the same OD scale for quantitative comparison, in the panel b, c, d, and e, respectively. RNA is likely to be localized in the nucleolus. Actin is known as one of nuclear proteins as well as cytoplasmic cytoskeletal protein. Although the present analysis is preliminary, because residual molecules are found to exist with significant quantity, the result indicated that the present preparation of the thin section with paraffin for imaging nucleus will be successful. Analysis including paraffin spectra is in progress.

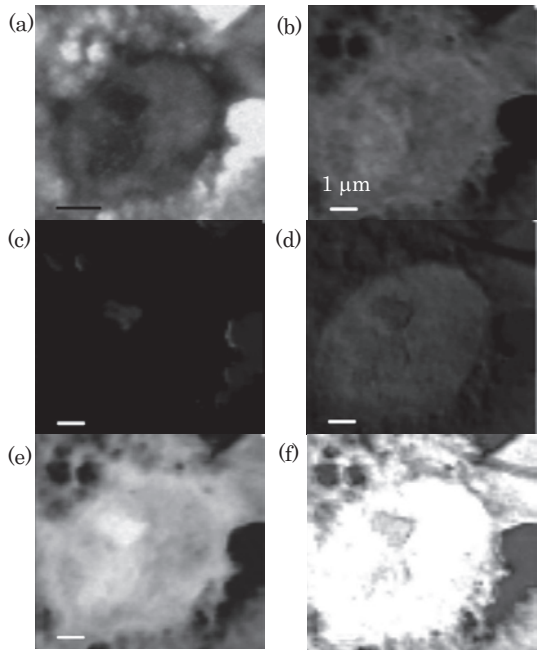

Fig. 1. Molecular distributions in an isolated human nucleus. (a) X-ray image at 285 eV, (b-e) molecular distribution of DNA, RNA, histone and actin, (f) residual molecules.

[1] K. Shinohara *et al*., Ultramicrosc. **194** (2018) 1.
[2] K. Shinohara *et al.*, J. X-Ray Sci. Technol. **26** (2018) 877.
[3] K. Shinohara *et al.*, Cells **8** (2019) 164.
[4] A. Ito *et al*., UVSOR Activity Report **48** (2020) 130.

BL4U

Investigation of the Terrestrial Weathering Process of Ryugu Grains

M. Miyahara[1] and T. Araki[2]

[1]*Graduate School of Advanced Science and Engineering, Hiroshima University, 1-3-1 Kagamiyama, Higashi-Hiroshima, Hiroshima 739-8526, Japan*

[2]*UVSOR Synchrotron Facility, Institute for Molecular Science, Okazaki 444-8585, Japan*

Ryugu grains, which are collected from the asteroid Ryugu, mainly consist of saponite, serpentine, magnetite, sulfides, carbonates, and phosphates, closely resembling CI-group carbonaceous chondrites [1]. CI chondrites are highly susceptible to terrestrial weathering, making it difficult to study their original features. Even Antarctic meteorites, despite better preservation, experience long exposure to water and ice. To understand early-stage terrestrial weathering of CI chondrites, this study proposes to expose Ryugu grains to atmospheric conditions and monitor surface changes, providing insights into weathering processes not possible from meteorites alone.

The sample plate C0105-042, previously analyzed by the Hayabusa2 Initial Analysis "Sand" Team, was used in this study [2]. It contains small Ryugu grains from chamber C of the second touchdown. After allocation by JAXA, over 24 grains were mounted onto C0105-042 with minimal epoxy in an N_2-filled glove box. Following approval of our terrestrial weathering AO proposal, the sample plate C0105-042 was sent to Hiroshima University. The sample plate C0105-042 was exposed to air in a desiccator. FE-SEM observations were done 104 and 245 days after exposure began. For TEM and STXM analysis, ultrathin foils were prepared using a FIB system. TEM observations and SAED pattern analysis were conducted for structural and chemical analysis, with quantitative EDS analysis. STXM analysis was conducted at BL4U, UVSOR Synchrotron facility to analyze C K-, S L-, and Fe L-edges using energy stacking methods. Elemental maps and NEXAFS spectra were processed using aXis2000.

FE-SEM observations of the C0105-042 Ryugu grains showed significant surface changes after exposure experiments. Cracks widened, some grains fragmented, and fine-grained precipitates (Fig. 1a) formed on mineral surfaces. Pyrrhotite surfaces were entirely covered by amorphous, amoeboid precipitates (Fig. 1b), obscuring their original outlines. With longer atmospheric exposure, precipitate sizes increased (>200–300 nm), and cracked grains detached completely. TEM analysis revealed that these precipitates were mostly amorphous, carbon- and oxygen-rich layers about 100 nm thick. The amoeboid precipitates on pyrrhotite were iron- and sulfur-depleted, oxidized or hydrated.

Based on the Fe L_3-edge XANES spectra, Fe^{2+} is dominant in the pyrrhotite ($Fe_{1-x}S$)-dominated regions, whereas Fe^{3+} is dominant in the saponite–serpentine matrix. S L-edge XANES spectrum indicate that at pyrrhotite-dominated regions, minor absorption peaks appear around 162 eV and 164 eV (Fig. 1c), corresponding to S^{2-} and elemental sulfur (S^0), respectively [3, 4]. Additionally, a broad absorption band between 167–174 eV is observed (Fig. 1c), attributed to oxidized sulfur species such as S^{4+} and S^{6+} [4]. C K-edge XANES spectrum show that at saponite–serpentine matrix that include carbonaceous material an absorption near 290.5 eV is observed, corresponding to carbonate (CO_3^{2-}) groups [5]. The absorption peak corresponding to the carbonate becomes weaker and an absorption peak corresponding to the C=C bond appears instead as the fine-grained precipitate layer is close to the surface of minerals

Considering the TEM observations and STXM analysis, the terrestrial weathering of Ryugu grains is initiated by the natural oxidation of pyrrhotite. It is highly probable that pyrrhotite reacts with atmospheric moisture, leading to the oxidation of sulfur into sulfate ions, which in turn may cause the decomposition of surrounding saponite, serpentine, and carbonaceous materials. The mechanism and rate by which sulfur leached from pyrrhotite affects these adjacent materials are currently under investigation.

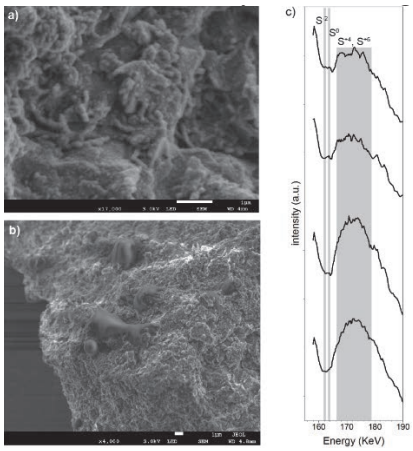

Fig. 1. SE images of a) fine-grained precipitates and b) amoeboid precipitates and c) Representative S L-edge XANES spectrum.

[1] T. Nakamura *et al*., Science **379** (2023) eabn8671.
[2] T. Noguchi *et al*., Nat. Astron. **7** (2023) 170.
[3] S. P. Farrell *et al*., Am. Mineral. **87** (2002) 1321.
[4] D. Li *et al*., Can. Mineral. **33** (1995) 949.
[5] J. A. Brandes *et al*., J. Synchrotron Radiat. **17** (2010) 676.

BL4U

Inorganic Nitrogen in Springtime Aerosol Particles over the Arctic Ocean

N. Fauré[1], T. Araki[2], R. Pohorsky[3], G. P. Freitas[4], J. Schmale[3], P. Zieger[4], J. Creamean[5], E. S. Thomson[1] and X. Kong[1]

[1]*Department of Chemistry and Molecular Biology, University of Gothenburg, Gothenburg SE-412 96, Sweden*
[2]*UVSOR Synchrotron, Institute for Molecular Science, Okazaki 444-8585, Japan*
[3]*Extreme Environments Research Laboratory, EPFL, Sion 1950, Switzerland*
[4]*Department of Environmental Science, Stockholm University, Stockholm SE-106 91, Sweden*
[5]*Department of Atmospheric Science, Colorado State University, Fort Collins CO 80523, USA*

The Arctic region is warming at a rate two to four times faster than the global average, a phenomenon known as Arctic Amplification (AA). Aerosol particles play an important role in this accelerated warming. However, the extent of their impact depends on their physicochemical properties (e.g., chemical composition, size, and hygroscopicity). [1] Here, we utilize STXM/NEXAFS to investigate the chemical composition of both ambient and laboratory-generated Arctic springtime aerosol particles. These aerosol particles were collected during the Atmospheric Rivers and the Onset of Sea Ice Melt (ARTofMELT) expedition, which took place in the Fram Strait from May to June 2023 onboard the Swedish icebreaker Oden. Ambient aerosol particles were collected at surface level (at sea ice edge) and in clouds at higher altitudes (with a tethered balloon). Laboratory-generated aerosol particles were produced using a Sea Spray Chamber (SSC) onboard the vessel, which was filled with freshly collected seawater and melted snow.

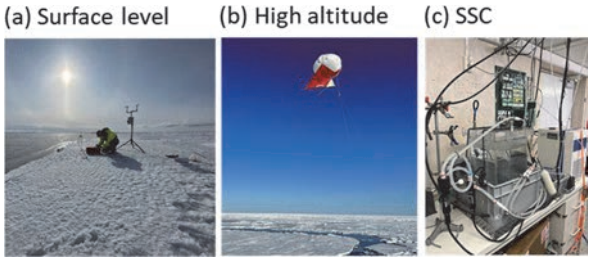

Fig. 1. Ambient aerosol particles collected (a) at the sea ice edge, (b) with a tethered balloon, and (c) from a SSC used to generated sea spray aerosol particles.

The STXM/NEXAFS results reveal that ambient aerosol particles are dominated by ammonium sulfate ($(NH_4)_2SO_4$) and sodium nitrate ($NaNO_3$), while the laboratory-generated sea spray aerosol particles are dominated by sodium chloride (NaCl). The discrepancy between the ambient aerosol particles and those generated using the SSC highlights the potential influence of different sources and formation mechanisms in the ambient environment. Notably, no chloride was detected in ambient particles, suggesting an impact of aging processes on sea spray aerosol compositions, such as dichlorination via acid replacement with nitric acid (HNO_3) and the emission of hydrogen chloride (HCl). [2] Further analysis will be conducted to better understand the different sources and mechanisms at play.

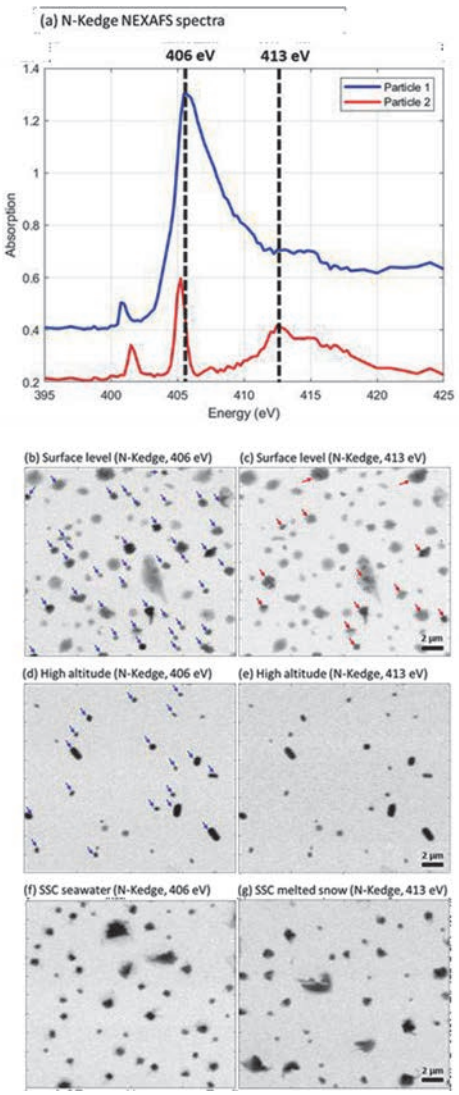

Fig. 2. (a) Nitrogen K-edge NEXAFS spectra with ammonium absorption edge (406 eV) and nitrate absorption edge (413 eV). Overview scans for particles collected (b-c) at surface level close to the sea ice edge, (d-e) at higher altitudes in cloud with a tethered balloon, (f) with the seawater filled SSC and (g) from the SSC filled from melted snow. Blue arrows correspond to particles containing ammonium, red arrows to particles containing nitrate and no arrows to particles with other compositions.

[1] J. Schmale *et al.*, Nat. Clim. Change. **11** (2021) 95.
[2] B. Su *et al.*, Atmos. Environ. **290** (2022) 119365.

BL4U

Investigating Ti-organometallic Complexes Found in Mars-relevant Mineral- microbial Interfaces Exposed Outside the ISS as Potential Biosignatures in the Search for Life on Mars

M.C. Sforna[1] and T. Milojevic[1]
[1]*Center of Molecular Biophysics, CNRS – University of Orleans, Orleans, France*

Searching for traces of life is the core of Mars exploration as conditions were reunited on early Mars for the appearance of Life. Chemolithotrophs (rock-eating microorganisms) may have been predominant on early Mars [1], but the understanding of their putative biosignatures in Martian materials is limited. We investigated *Metallosphaera sedula*, an ancient extremophilic archeon that extracts energy from diverse inorganic electron donors, and which has the particularity to induce specific biomineralization patterns depending of the substrate, which may be preserved for billions of years [2, 3]. *M. sedula* cells were grown on the 4.5 Gyrs-old NWA7034 meteorite [2], and exposed for one year outside of the International Space Station under Martian conditions within the framework of the Japanese Tanpopo-4 orbital project [4, 5]. Preliminary analyses on the retrieved cells showed that despite the abundance of Ti-oxides in NWA7034 [6], there were no traces of Ti- oxides after microbial growth, both in the exposed and in the ground control samples, ruling out photoionization processes. This transformation of Ti- oxides is intriguing, as Ti-oxides are known to be excellent catalyzers for chemical reactions, but, there are no reports of their role on bioprocesses [7]. One question arose from these results: could Ti- organometallic compounds be a suitable signature for the search of life on Mars?

To answer this question, we performed, in May and in October 2024, STXM and XANES spectroscopy at C K-edge, N K-edge, S L-edge and Ti L-edge on the BL4U beamline on exposed and ground control (GC) cells to (1) confirm that Ti accumulation in close proximity with cells is really an organometallic compound, (2) better identify the organometallic complex(es), (3) understand if this complex is preserved under Martian conditions by comparing ground control and ISS-exposed cells, and then to (4) assess Ti-organometallic complexes as potential biosignatures.

In May 2024, we investigated 2 ultra-thin sections of IS cells and ultra-thin section of GC cells, embedded in epoxy resin and deposited on TEM grids. We performed 176 images at the C K-edge and the Ti L- edge, and 25 scans in energy across the C K-edge and the Ti L-edge. In October 2024, we analyzed cells directly dropped on Si3N4 windows (4 windows for ISS, 2 for GC), and were able to better examine the change on the cells resulting from spatial exposure. We performed 141 images at the C K-edge, N K-edge, S L-edge and Ti L-edge, and 47 energy scans, mostly across the C K-edge and the S L-edge.

STXM and XANES at the Ti L-edge did not evidence the presence of Ti-organometallic compounds, but only showed the presence of nanophases of anatase and rutile associated to the cells, suggesting that the transformation of Ti-minerals is not as complete as previously thought.

Our experiment also allowed to investigate the damages on the molecular composition of the cells underwent during ISS exposition. The C K-edge spectra for GC cells show three main bands centered at ~285.1, 287.6 and 288.5 eV, indicating a mixture of biomolecules within *M. sedula*, with prominent lipids, proteins and saccharides features, with a particularly high lipid contribution compared to general composition of cells [8]. Overall, a higher hydroxylation of the functional groups can be observed in the ISS exposed cells compared to GC cells, supported by a globally stronger carboxylic signal, more defined hydroxylated aliphatic peak and carbonyl peaks, and weaker bands for the ketone/phenol/nitrile absorption region. The S L-edge spectra performed on GC and in exposed cells show similar spectra with two main bands, centered at ~173 and ~182 eV spectra, suggesting a +6 redox state for S, most certainly contained in sulphates [9], suggesting a good preservation of the sulfates. The higher hydroxylation is a common features in cells when exposed to UV. Indeed, UV radiation is known to be damageable for cells, increasing the amount of reactive oxygen species in the cells and hydroxylating the functional groups [10, 11]. However, the presence of sulphates not degrading under UV could have limited this damaging action, and allowed their survival under these conditions. These results are included in an article in review.

[1] J.P. Grotzinger *et al*., Science **343** (2014) 12427777.
[2] J.Guo *et al*., Astron. J. **155** (2018) 49.
[3] T. Milojevic *et al*., Commun. Earth Environ. **2** (2021) 39.
[4] D. Kölbl *et al.,* Front. Microbiol. **8** (2017) 1918.
[5] Y. Kawaguchi *et al*., Front. Microbiol. **11** (2020) 2050.
[6] T. Milojevic *et al.,* EGU **23** (2023) 16175.
[7] AR Santos *et al*., Geochim. Cosmochim. Acta **157** (2015) 56.
[8] MR Zierden and AM Valentine. Metallomics **8** (2016) 9.
[9] L.Z. Liu *et al.,* Res. Microbiol. **169** (2018) 590.
[10] G. Sarret *et al*., Geochim. Cosmochim. Acta **63** (1999) 3767.
[11] J. Cadet, J. and J.R. Wagner, J. R. Cold Spring Harbor Perspect. Biol. **5** (2013) a012559.

BL4B

Development of XANES Imaging Method for Visualizing Intracellular Chemical Species

R. Sasaba[1,2] and H. Iwayama[2]
[1]*Graduate School of Frontier Biosciences, The University of Osaka, Suita 565-0871, Japan*
[2]*UVSOR Synchrotron Facility, Institute for Molecular Science, Okazaki 444-8585, Japan*

Detecting the distribution of intracellular molecules or chemical components is very important. Several imaging methods to visualize them, such as Raman microscopy, have been proposed so far. Since the spectral structures of X-ray Absorption Near Edge Structure (XANES) spectroscopy depend on the chemical species, we are developing a XANES imaging method to visualize the distribution of chemical species within a cell using contact-type soft X-ray microscopy [1].

In this method, we measure transmitted X-ray images of biological samples at K- or L-edge energies of elements such as carbon, sulfur, and iron. Biological samples are placed on a Ce:YAG scintillator and covered with a 100 nm-thick Si_3N_4 membrane. The transmitted X-ray image is converted into a visible light image by the scintillator, and then captured by a CMOS camera. By changing photon energies, we can obtain photon-energy dependence of transmitted images Is(X, Y, E), where X and Y represent the positions of the camera and E is a photon energy, respectively. We also measure blank data I_0(X, Y, E) without the sample. From the Lambert-Beer law, we can obtain a three-dimensional XANES image (X, Y, E) from I_0(X, Y, E) and Is(X, Y, E).

The experiment was performed on the beamline BL4B at UVSOR-III. Figure 1 shows the observation result of a human oral epithelial cell using our contact-type soft X-ray microscopy and XANES spectra at four different positions (X,Y) on the sample. Each of the four XANES spectra is different. The No. 1 XANES spectrum corresponds to a cell-free region and consistently shows values close to zero, indicating the background of the spectroscopy. The No. 2 spectrum corresponds to the edge of a cell and exhibits a strong peak around 287 eV. The No. 3 spectrum, taken from the inner region of the cell, shows two peaks at approximately 285 eV and 287 eV. The No. 4 spectrum, acquired from the center of the cell, also exhibits two peaks; however, their intensities are significantly different.

After normalizing all XANES spectra, we extract some feature values from XANES spectra using machine learning techniques. Figure 2 shows the results of these feature calculations. Figure 2(a) displays the peak area around 285 eV, which reflects the amount of aromatic compounds. Figure 2(b) shows the peak area around 287 eV, corresponding to alkyl groups. Figure 2(c) represents the ratio between the peaks at 285 eV and 287 eV, providing contrast related to the relative abundance of aromatic and alkyl compounds. Figure 2(d) shows the spectral difference around 295-320 eV.

These visualized features help us to distinguish different regions within the cell based on their chemical compositions. For example, we could now know how aromatic compounds distribute within a cell.

We are currently working on applying this method to various types of biological samples, such as MDCK cells.

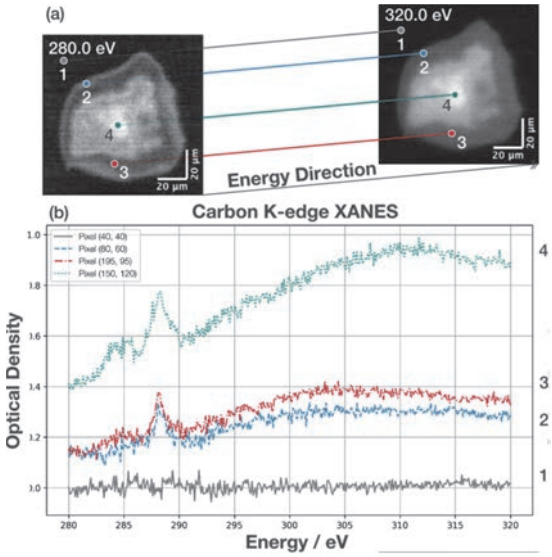

Fig. 1. The imaging result of a human oral epithelial cell using contact-type soft X-ray microscopy and XANES spectra at four different pixels.

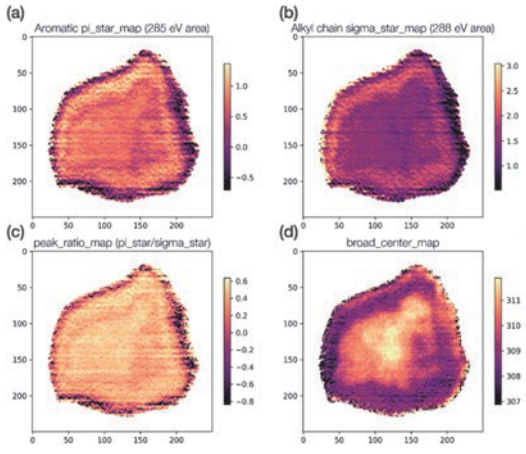

Fig. 2. Maps of spectral features calculated from individual XANES spectra at each pixel position.

[1] T. Ejima *et al.*, J. Phys.: Conf. Ser. **463** (2013) 1.

BL7B

Investigation of Space Weathering Effects on PAHs Using Laboratory Simulations

C. Wu[1], S. Liu[1], K. Yoshioka[1] and I. Yoshikawa[1]
[1]*Department of Complexity Science and Engineering, Graduate School of Frontier Sciences, The University of Tokyo, Chiba 277-8561, Japan*

Polycyclic aromatic hydrocarbons (PAHs) are widespread cosmic organic molecules. The PAH hypothesis indicates a 217.5 nm absorption bump of the interstellar extinction curve may be attributed to the PAH molecule. This theoretical hypothesis was supported by an experiment of Joblin et al. [1] Additionally, space weathering refers to the physical and chemical changes that occur on the surfaces of airless bodies or objects when exposed to interplanetary environments, resulting in alterations to their spectroscopic features. One significant effect should be noted, this process may cause absorption bands to shift towards longer wavelengths after exposure. There are various approaches to studying space weathering, including the early analysis of Apollo samples and subsequent irradiation experiments conducted on the International Space Station. Among these methods, laboratory simulations of space weathering have become a widely used research technique.

In this study, we employed UV irradiation experiments using 0th-order light on coronene. Subsequently, we utilized beamline BL7B to measure the transmittance spectra of the samples exposed to 0th-order light and unexposed.

In the irradiation experiments, coronene samples were subjected to irradiation for durations of 3 hours, 6 hours and 8 hours, utilizing the 0th-order light from BL7B.

In the transmittance spectra measurement experiment, a photodiode was utilized. The detailed experiment structure can be seen in Fig.1. Additionally, for reducing the effect of higher-order light to obtain more accurate results, various gratings and filters combinations were utilized. Specifically, the setups included the G2 grating plus Quartz and Pyrex filters, as well as G3 grating plus Quartz and Pyrex filters.

In calculating absorption spectrum, due to samples and substrates being too thin, which causes the reflectance to be negligible compared to the transmittance. Therefore, the absorption ratio can be calculated by 100% minus the transmittance ratio. Consequently, the absorption spectrum in Fig.2 can be obtained.

According to the results on Fig. 2, the absorption spectrum has altered after 3-hour and 8-hour of 0th-order light irradiation, compared to the spectrum without irradiation. The detailed performance is peak shift towards shorter wavelengths. The reason for peak shift was considered the hydrogen atom loss.

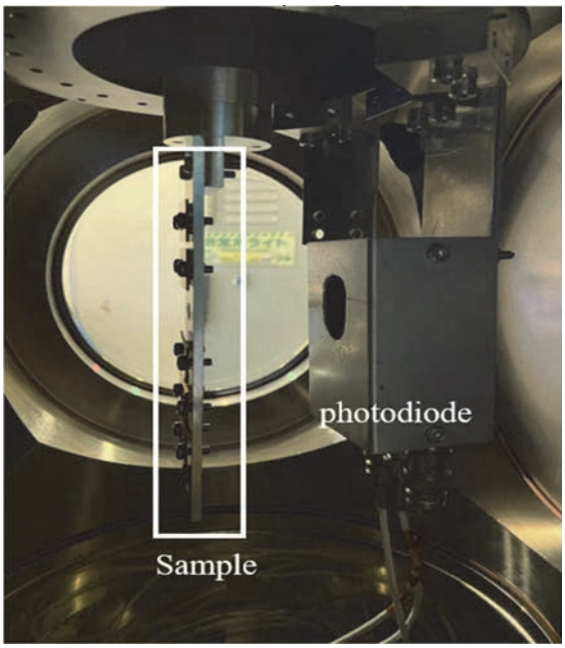

Fig. 1. Spectra measurement experiment.

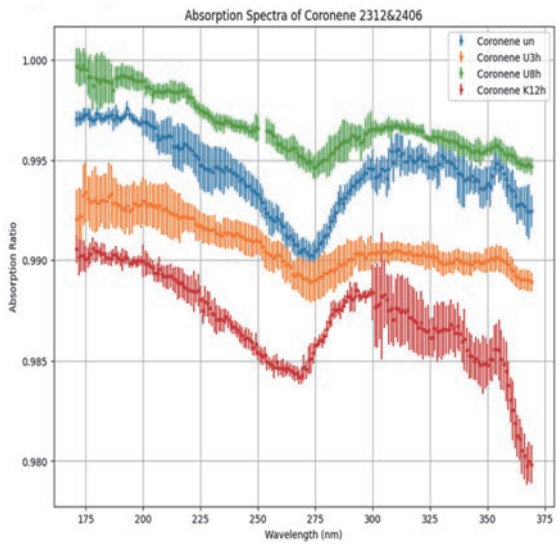

Fig. 2. Absorption spectra of coronene exposed and unexposed.

[1] C. Joblin *et al*., Astrophys. J. **393** (1992) L79.

III-5

UVSOR User 14

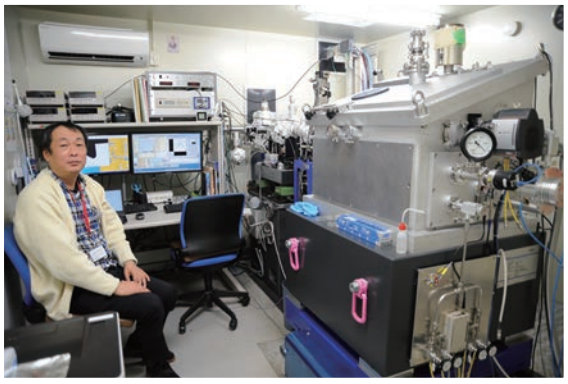

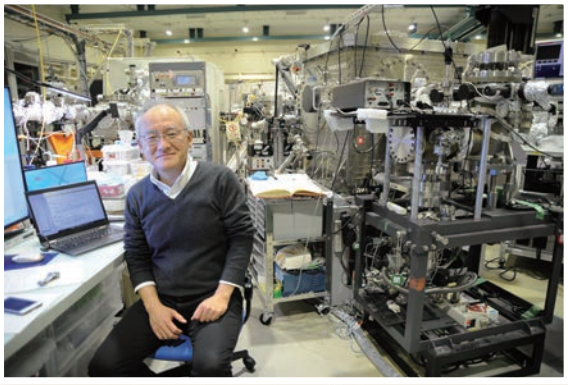

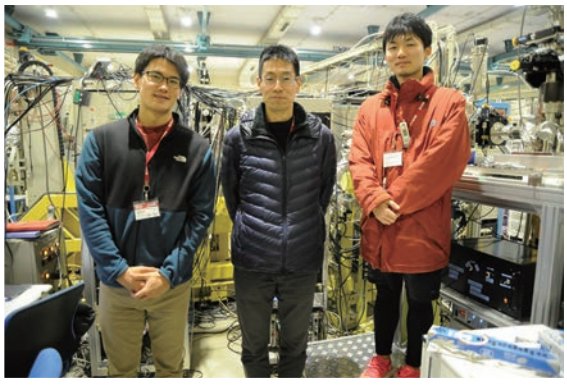

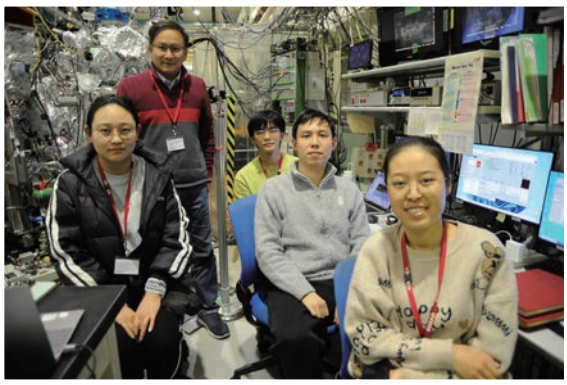

UVSOR User 15